



**HAL**  
open science

## **Radiation tolerance assessment of COTS components for an optoelectronic system to measure polymer aging in nuclear environments**

Mohamed Iheb Boussandel, Ahmed Fathallah, Jean-Marc Armani, Faouzi Armi, Mohamed Ben Chouikha

### ► To cite this version:

Mohamed Iheb Boussandel, Ahmed Fathallah, Jean-Marc Armani, Faouzi Armi, Mohamed Ben Chouikha. Radiation tolerance assessment of COTS components for an optoelectronic system to measure polymer aging in nuclear environments. RADECS 2023 - Radiation and its Effects on Components and Systems, Sep 2023, Toulouse, France. 2023, RADECS2023 Conference Proceedings. cea-04789672

**HAL Id: cea-04789672**

**<https://cea.hal.science/cea-04789672v1>**

Submitted on 18 Nov 2024

**HAL** is a multi-disciplinary open access archive for the deposit and dissemination of scientific research documents, whether they are published or not. The documents may come from teaching and research institutions in France or abroad, or from public or private research centers.

L'archive ouverte pluridisciplinaire **HAL**, est destinée au dépôt et à la diffusion de documents scientifiques de niveau recherche, publiés ou non, émanant des établissements d'enseignement et de recherche français ou étrangers, des laboratoires publics ou privés.

# Radiation Tolerance Assessment of COTS Components for an Optoelectronic System to Measure Polymer Aging in Nuclear Environments

M. I. Boussandel, A. Fathallah, J. M. Armani, F. Armi and M. B. Chouikha

**Abstract**—The radiation dose tolerance of several microcontrollers, LED drivers and differential amplifiers was tested using 60Co gamma-rays. We found that the tested devices are tolerant up to a dose comprised between 130 and 1000 Gy.

**Index Terms**—Infrared, Light Emitting Diodes driver, Microcontroller, Operational Amplifier, Polymer Aging, Total Ionizing Dose.

## I. INTRODUCTION

**P**OLYMERS are widely used in Nuclear Power Plants (NPPs) as protective, sealing or isolating coatings in a lot of equipment such as electrical cables and pipes. These materials play a crucial role for safety and security of NPPs [1]. Constant monitoring of polymer aging is therefore mandatory.

Assessment of polymer degradation and aging check operations are usually performed using destructive techniques. Although this invasive method is reliable, it is expensive and time consuming [1] [2] [3].

A new polymer aging detection system has been developed and validated in the framework of a previous collaboration work [4]. The principle of noninvasive detection used is based on the measurement of variations in polymer's absorbance at a set of wavelengths specific to the aging.

This research work continues within the framework of the European project 945320 El-Peacetolero. The main objective of this European project is to design a TRL 7 portable, low-power, optoelectronic system for in-situ and real-time identification of polymers, and diagnosis of the material state of aging in an industrial environment.

The architecture of the proposed optoelectronic system is depicted in figure 1. It is composed of infrared (IR) sources, which can be light emitting diodes (LEDs) and/or Laser diodes, with their driver circuitry, IR photodetectors, Thermo-Electrical Cooling (TEC) circuits to control IR devices temperature, an analog circuit for the readout of the detector photocurrent, analog to digital converter (ADC), and advanced data processing & analysis unit.

Manuscript received April 7, 2023.

J. M. Armani is with Université Paris-Saclay, CEA, List, F-91120, Palaiseau, France, (e-mail: jean-marc.armani@cea.fr).

M. I. Boussandel, A. Fathallah, F. Armi and M. B. Chouikha are with Sorbonne Université, CNRS, Laboratoire de Génie Electrique et Electronique de Paris, 75252, Paris, France, and with Université Paris-Saclay, CentraleSupélec, CNRS, Laboratoire de Génie Electrique et Electronique de Paris, 91192, Gif-sur-Yvette, France, (e-mail: mohamed.ben\_chouikha@sorbonne-universite.fr).

We made the choice of using commercial off-the-shelf (COTS) components to develop and design the embedded optoelectronic system. As a matter of fact, the design of an application specific integrated circuit (ASIC) for the embedded system would exceed the project goals and timing.

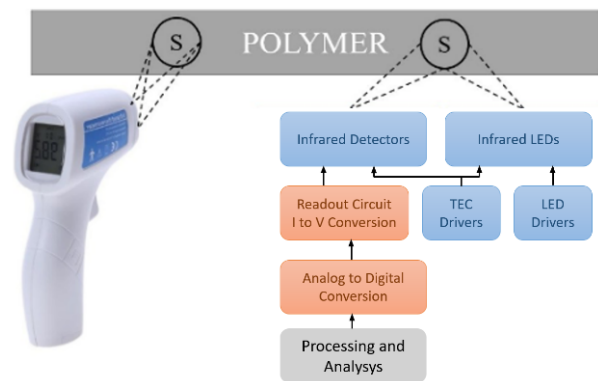


Figure 1. Architecture of El-Peacetolero embedded optoelectronic system.

As the embedded system is meant to be exploited in nuclear facilities it will be exposed to large variety of radiation levels depending on the maintenance needs. Therefore, it should be designed to be radiation tolerant, i.e. hardened to the effects of ionizing dose.

## II. SYSTEM DESIGN AND COMPONENT SELECTION

### A. Hardness Requirement

The embedded optoelectronic system could be used to perform aging measurement on pipes or insulating polymers of electric cables in a NPP. Accordingly, a typical mission scenario has been defined to specify the required radiation hardness level for the embedded optoelectronic device. It defines a use case where the embedded device is mounted on a robot and deployed in a reactor building. In this environment, the ambient temperature and the gamma dose rate can reach 50 °C and 0.1 Gy/h when the reactor is in operation.

We made the following assumptions for defining the scenario: the duration of a measure is around 1 minute per cable; the robot will have to check about 600 cables per mission. Therefore, considering the maximum dose rate mentioned above, the total ionizing dose absorbed by the device will reach 1 Gy during a mission. If we expect an operating life of 20 years and an interval of one year between two measurement

campaigns, we will have a cumulated dose of 20 Gy over this lifetime. Based on this value, we have set to 100 Gy the required TID hardness level for the embedded system in order to have a sufficient safety margin.

### B. Selection of components

A first design of the system, called “original design”, has been realized selecting COTS components that reach the system specifications. In order to maximize the chances of finding components that meet hardness requirement for missions in NPPs, we selected for each electronic part of the original design an alternative reference that is electrically and functionally equivalent. When possible, the alternative reference was chosen from a manufacturer other than the original one. This paper presents the irradiation tests results of the more significant components which are LED drivers, microcontrollers and differential amplifiers used in the design.

The infrared LEDs operate in pulsed mode and it is recommended to drive them at 1kHz frequency. In order to maximize the power output to its limit, a duty cycle of 2% (20  $\mu$ s pulse) must be applied at 1A driving current [5]. The current driver STCS1 and STCS2 from STMicroelectronics meet these requirements thanks to their response time and stability.

The microcontroller’s embedded ADC must have at least 1 MSPS sampling rate and 16-bits resolution in order to achieve 20 samples during the IR pulse and quantify the minimum polymer absorbance induced by aging. The selected microcontrollers are the C8051F060 from Silicon Labs and the OSD32MP157C from Octavo System. Both include two SAR-ADCs and allow differential mode operation.

Differential amplifiers must improve the ADC dynamic range. Their noise must also satisfy the 16-bit ADC resolution. The selected amplifiers are the THS4503CDG from Texas Instruments and the AD8132ARZ from Analog Devices. Several previous works have evaluated the radiation tolerance of classical operational amplifiers [6] [7]. To our knowledge, no previous paper deals with these particular components.

## III. EXPERIMENTAL PROTOCOL

### A. Test procedure

A specific test bench has been manufactured for the irradiation of electronic components. For each part, this bench provides online monitoring of key electrical parameters that have been previously chosen. It is made up of several test boards, instrumentation devices for measuring electrical signals and a PC which controls the measurement and saves the results. For each component, a mezzanine board was designed and fabricated. Two sets of these boards were irradiated in order to have data on two samples of each component and thus to have an idea of the dispersion. During the irradiation phase, the bench was configured to perform measurement of the components with an interval period of 15 minutes.

Additional pre- and post-irradiation characterization tests were conducted to assess the performance of the selected devices. The tests included evaluation of proper working of the microcontroller’s internal peripherals involved in the acquisition process, such as RAM, ADCs, timers, and output pins.

Frequency response and current consumption measurements were used to assess the performance of differential amplifiers.

For STCS1 and STCS2 LED drivers, functionality tests performed aimed to determine the response time, offset current, output current stability and accuracy.

### B. Irradiation

All components were irradiated in the IRMA facility, a  $^{60}\text{Co}$  irradiation cell located at the CEA Saclay research center (France). This facility is used to study the effects of gamma radiation on equipment or materials. The IRMA cell has several high activity  $^{60}\text{Co}$  sealed sources, the number of which can be adapted according to the desired dose rate. At the time of starting the experiment, the total activity of the sources was 511 TBq and the maximum available dose rate was around 7.6 kGy/h at 10 cm.

Figure 2 shows the test boards during their installation in the irradiation cell. A common dose rate of 24 Gy/h was used during the test in order to obtain an accumulated dose of 1 kGy after an irradiation period of 42 hours.

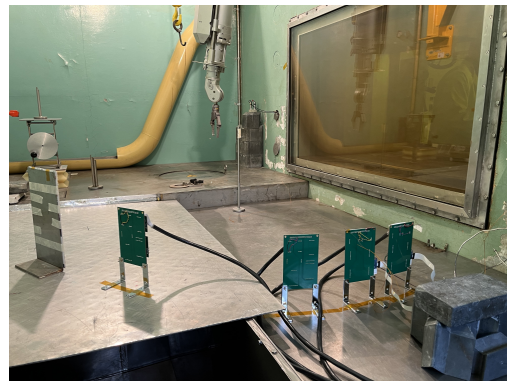


Figure 2. Test boards in the irradiator before starting the experiment.

## IV. RESULTS & DISCUSSION

### A. Characterization results

1) *LED drivers*: The goal of the characterization tests was to evaluate for the LED drivers STCS1 and STCS2 the performance degradation induced by radiation. The tests before irradiation have led to the following results:

Table I  
LED DRIVERS CHARACTERIZATION RESULTS

| Device | Resp. time  | Offset cur.   | Stability | Accur. |
|--------|-------------|---------------|-----------|--------|
| STCS1  | 2.4 $\mu$ s | $< 10^{-3}$ A | $< 1\%$   | 98%    |
| STCS2  | 2.5 $\mu$ s | $< 10^{-3}$ A | $< 1\%$   | 98%    |

After irradiation, the STCS1 and STCS2 current drivers were no longer operational and therefore we could not make any measurement. So we are not able to compare the characterization results for these components.

To circumvent this, a new experiment with some selected components will be planned this year. A full set of characterization tests will be carried out during planned stops of the irradiation in order to monitor the evolution of the above parameters.

2) *Microcontrollers*: The OSD32MP157c-512M-BAA is a SIP module based on the STM32MP157C microprocessor from STMicroelectronics which embeds some RAM and a power management unit IC STPMIC1. The STM32MP157C is composed of a dual core Arm Cortex A7 and Arm Cortex M4 coprocessor and a dedicated 3D graphics processing unit (GPU). This complex system run under Linux and thus has to be tested using system primitives for checking the functionality of each hardware feature.

We were able to test the embedded ADCs through Linux, by sampling a 520 mV DC signal injected on both ADC inputs. We did not observed significant degradation on the ADC conversion results.

Table II  
MICROCONTROLLERS CHARACTERIZATION RESULTS

| Feature         | Pre-irrad. | Post-irrad.          |
|-----------------|------------|----------------------|
| Linux boot      | No errors  | No errors            |
| STMMIC1A PMIC   | No errors  | No errors            |
| Cortex A7 & M4  | No errors  | No errors            |
| 3D GPU: Vivante | No errors  | No errors            |
| DDR3L Memory    | No errors  | No errors            |
| 16-bit ADC      | Ref. point | no significant degr. |

Those simple tests allowed for a basic testing of the OSD32MP157c-512M-BAA module. However, due to the project constraints and the large number of tested components, we decided for this first experiment to only check the functionality of the device and how much it can tolerate gamma radiation. A more rigorous characterization of the embedded ADCs of selected components will be realized during another irradiation that we will plan later this year.

3) *Differential Amplifiers*: Figure 3 shows the frequency response of the THS4503CDG and AD8132ARZ fully differential op-amps (FDAs). The Bode plot for the THS4503CDG input versus output shows a relatively flat frequency response up to 10 MHz, beyond which the gain starts to roll off.

The pre- and post-irradiation Bode plots of each FDA at worst case demonstrate some form of degradation. The negative output  $V_n$  of the AD8132ARZ shows a gain decrease, and the positive output  $V_p$  shows a flattened resonance peak and a decrease in roll-off rate starting at 10 kHz.

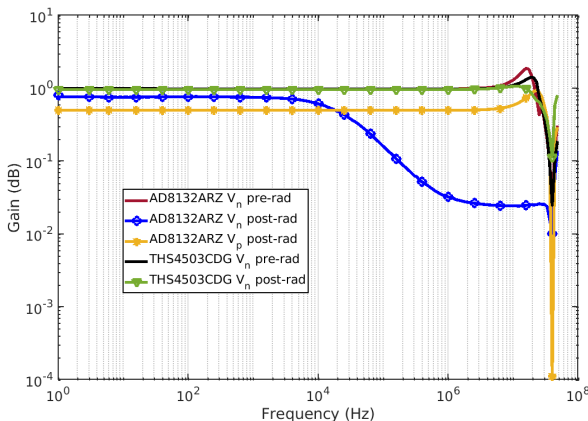


Figure 3. AD8132ARZ and THS4503CDG pre/post irradiation bode plot.

We also noticed a current consumption increase with both amplifiers, from 30.0 mA to 112.8 mA and from 41.1 mA to 77.8 mA, for AD8132ARZ and THS4503CDG respectively.

### B. On-line measurement results

1) *LED drivers*: Figure 4 shows the plots of the supply and output currents as functions of the accumulated ionizing dose for the STCS1 and STCS2 LED drivers. Left scale is for the supply current and right one for the output current. The step that can be observed on the yellow curve at 470 Gy corresponds to a planned irradiation stop.

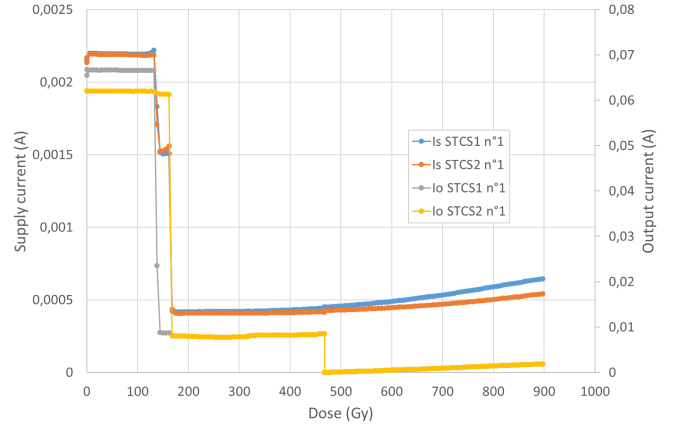


Figure 4. Response of STCS1 and STCS2 LED drivers during the irradiation.

Both components exhibit a fatal failure around 130 Gy which results in a sudden drop in the output current, from around 65 mA to 8 mA. After that moment, the two components remain non-functional until the end of the irradiation.

This early failure is most certainly due to the power supply that was applied continuously to the components during irradiation. These components are indeed manufactured with a BiCMOS process and a permanent polarisation is the worst case scenario for the CMOS part of their internal circuitry.

2) *Microcontrollers*: One can see on Figure 5 the plot of the power supply current and the conversion results of the two embedded ADCs (ADC0 and ADC1) for the C8051F060 and OSD32MP1 microcontroller modules. Left scale is for the supply current and right one for the output conversion code.

The C8051F060 microcontroller failed early after an accumulated dose of 180 Gy. From there, it stopped responding to requests from the PC and remained silent until the end of the test. As one can see, this failure has no impact on the current consumption of the component. This could mean that the degradation affect mainly certain internal functions of the component.

On the other hand, the OSD32MP1 module passed the irradiation test without failing but with some deviations in the ADCs conversion codes as one can see on Figure 5. The maximum variation observed below 100 Gy is 0.36%. The two ADCs produce the same code, which means that they probably use a common voltage reference. The observed deviations in the ADC output codes could be related to a degradation of this voltage reference.

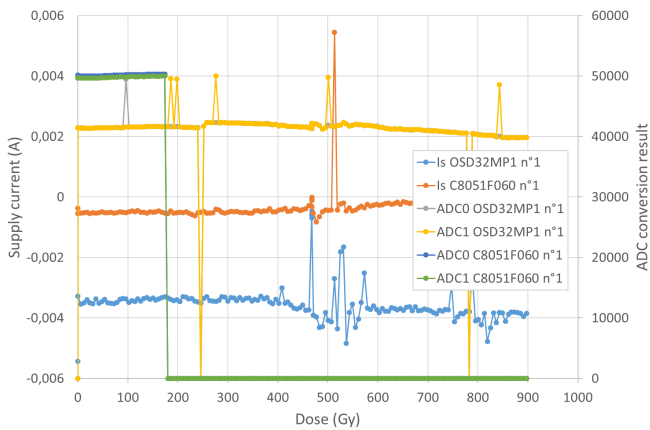


Figure 5. Response of OSD32MP1 and C8051F060 modules during the irradiation.

3) *Differential Amplifiers*: The plots of the supply currents and the output voltage of the THS4503 and AD8132 differential amplifiers are shown in Figure 6. The output voltage is measured with a constant voltage applied at the input of both amplifiers. All the amplifiers were configured with a unity gain for this measurement.

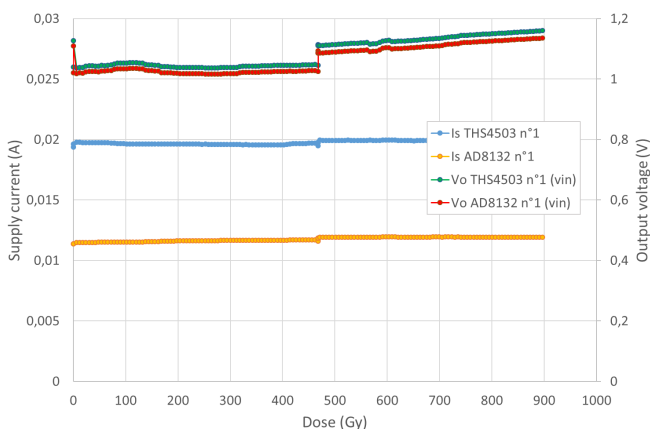


Figure 6. Response of THS4503 and AD8132 differential amplifiers during the irradiation.

One can see that the amplifier output voltages remain almost constant until 470 Gy when a step on the curves can be observed. As explained before this step corresponds to a planned irradiation stop at the halfway of experiment. The maximum variation of the output voltages below 100 Gy is 1.3%. The good stability of the signals means that the degradation of these bipolar components remains limited.

## V. CONCLUSION

The objective of this study was to find COTS components suited for the design of a hardened embedded optoelectronic device that can be operated in a NPP containment building to measure the aging of polymers. The required dose hardening of this system was set at 100 Gy. During this study, several

references of LED drivers, differential amplifiers, and microcontrollers have been irradiated up to 1 kGy with gamma rays to evaluate their tolerance to total ionizing dose.

The STCS1 and STCS2 LED drivers from STMicroelectronics failed early at a dose level of 130 Gy. These circuits have barely passed the test, so another components should be investigated.

The THS4503 and AD8132 differential amplifiers did not show significant degradation until the end of the test after an accumulated dose of 1 kGy. These bipolar components are already qualified for the design of the hardened system.

The C8051F060 microcontroller failed at 180 Gy. Even though this dose level is above our required limit, we will prefer the OSD32MP1 module which passed the test successfully without failure. This module showed however some deviation on the ADCs conversions.

This work was an preliminary study aimed at identifying candidate COTS components for the hardened optoelectronic system. Another irradiation test will be performed on the selected COTS components. During this future test, post-irradiation annealing will be also evaluated.

## ACKNOWLEDGMENT

The 945320 - El-Peacetolero - NFRP-2019-2020 project has received funding from the EUROPEAN COMMISSION, Directorate-General for Research and Innovation, Euratom Research, Innovation. El-Peacetolero started in Sept-2020 for 48 months. This publication reflects only the authors' view and the European Commission is not responsible for any use that may be made of the information it contains.

The authors would like to gratefully thank the staff of the IRMA facility, H. Houjeij and S. Poirier, for the support they provided during the irradiation test.

## REFERENCES

- [1] M. Broudin and M. B. Chouikha, "Methodologies for efficient and reliable npp polymer ageing management," *EPJ Nuclear Sci. Technol.*, vol. 8, p. 22, 2022. [Online]. Available: <https://doi.org/10.1051/epjn/2022013>
- [2] S. Hettal, S. Roland, K. Sipila, H. Joki, and X. Colin, "A new kinetic modeling approach for predicting the lifetime of ath-filled silane cross-linked polyethylene in a nuclear environment," *Polymers*, vol. 14, p. 1492, 04 2022.
- [3] S. Hettal, S. Roland, K. Sipila, H. JOKI, and X. Colin, "A new analytical model for predicting the radio-thermal oxidation kinetics and the lifetime of electric cable insulation in nuclear power plants. application to silane cross-linked polyethylene," *Polymer Degradation and Stability*, vol. 185, p. 109492, 01 2021.
- [4] R. C. Alejandro and B. C. Mohamed, "Portable device and method for estimating a parameter of a polymer," France Patent WO2018091631(A1), TW201827809 (A), FR3059104, May 25, 2018.
- [5] *LED34BS-2 Specifications*, IoffeLED, Ltd, 2013. [Online]. Available: <http://www.mirdog.spb.ru/Specifications/2013/LED34BS-2.pdf>
- [6] J. M. Armani, S. Blairon, and A. Urena Acuna, "Total ionizing dose response of commercial off-the-shelf microcontrollers and operational amplifiers," in *2020 European Conference on Radiation and Its Effects on Components and Systems (RADECS)*, 2020.
- [7] K. I. Tapero, A. S. Petrov, P. A. Chubunov, V. N. Ulimov, and V. S. Anashin, "Dose effects in cmos operational amplifiers with bipolar and cmos input stage at different dose rates and temperatures," in *2015 15th European Conference on Radiation and Its Effects on Components and Systems (RADECS)*, 2015, pp. 1–4.